Supplementary Material

Supplementary Methods

Data Release: The ABCD data repository grows and changes over time. We used the ABCD Study neuroimaging data from Release 2.0 (NDA Study 634, DOI http://dx.doi.org/10.15154/1503209 accessed on 05/13/2019). All questionnaire data used in this study was updated with the Fix Release 2.0.1 (NDA Study 721, DOI 10.15154/1504041 accessed on 08/01/2019). An error in the orientation of the structural MRI data and field map correction in 26 participants became apparent in ABCD data release 2.0.1. These data were corrected and re-released in ABCD release 3.0 (NDA Study 901, DOI 10.15154/1519007 accessed on 11/05/2020. We downloaded the corrected neuroimaging data and preprocessed all subjects identically.

Functional Connectivity Quality assessments: Data were checked for correlations between mean motion and functional connectivity and between mean motion and functional connectivity distance dependence, based on recent recommendations (1). Before denoising, the average correlation across subjects/sessions between functional connectivity and mean motion was r = -0.08 +/- 0.06. After denoising this correlation was reduced to r = 0.01 +/- 0.06 (Supplementary Fig 2). Before denoising there was a strong correlation between functional connectivity and distance (r = 0.49 +/- 0.23), and after denoising this association was reduced (r = 0.01 +/- 0.19) (Supplementary Fig 3). We then checked for group differences in mean motion and number of frames remaining after censoring obtained from the CONN toolbox. There were no significant differences in the number of censored frames (new multisite pain: 124.63 +/- 84.46; MC: 116.71 +/- 79.67; p = 0.39) or in absolute mean motion (new multisite pain: 0.014 +/- 0.012; MC: 0.015 +/- 0.025; p = 0.61).

Structural Image Preprocessing: Within the fMRIPrep pipeline, the T1-weighted (T1w) image was non-uniformity corrected, skull-stripped (ANTs 2.2.0 (2)), and brain surfaces were reconstructed using recon-all (FreeSurfer 6.0.1 (3)). Spatial normalization to the ICBM 152 Nonlinear Asymmetrical template version 2009c was performed through nonlinear registration with antsRegistration (ANTs 2.2.0 (2)), using brain-extracted versions of both T1w volume and template. Brain tissue segmentation of cerebrospinal fluid (CSF), white-matter (WM) and gray-matter (GM) was performed on the brain-extracted T1w using fast (FSL 5.0.9 (4)).

Cortical Thickness
Outputs of recon-all were used for cortical thickness assessment, calculated as the distance between the gray/white matter boundary and the gray matter/CSF boundary at each vertex on the tessellated surface (3). Surface cortical thickness data smoothed using 2D surface smoothing (10 mm FWHM, mris_preproc), which was then entered into a whole-brain, vertex-wise GLM (mri_glmfit). Multiple comparisons correction was performed cluster-wise at $p < 0.05$ using mri_glmfit-sim.

Voxel Based Morphometry
Unwarped structural images were segmented using the "new segment" function in SPM12 running on MATLAB R2017a. The GM and WM images were then processed using the diffeomorphic

anatomical registration through exponentiated lie algebra (DARTEL) toolbox (5). From these images, DARTEL creates a high resolution average template, and the subject level GM images are aligned to match this template and then normalized to MNI space. The images were modulated to maintain the total amount of GM as the original images. Finally, the normalized and modulated GM images were smoothed with an 8mm FWHM kernel. Next, smoothed GM images were entered into a two-sample t-test analysis using the general linear model within SPM12. Total intracranial volume (sum of GM, WM and CSF) was included as a covariate of no interest. An absolute threshold mask of 0.1 (i.e. voxels with GM values <0.1 were excluded from analysis) was applied to avoid possible edge effects around the border between GM and WM, and to include only relatively homogeneous voxels. A voxel-level threshold of $p < 0.001$ was applied to all contrasts and results were deemed significant at the cluster level $p < 0.05$ false discovery rate (FDR) corrected for multiple comparisons.

Supplementary Figures

Supplementary Figure 1:
Participants were excluded if they had missing clinical or imaging data, or if the neuroimaging (structural or resting state) did not pass ABCD's recommended quality control metrics (see Imaging Instruments Release Notes https://nda.nih.gov/study.html?id=721). Briefly, this excluded subjects whose images were referred for clinical radiological review, showed bad structural or poor FreeSurfer reconstruction, and had less than 5 minutes of quality resting state data. To exclude sources of dependence, if multiple children from one family participated in the study, we used only the first enrollee. For these reasons, n = 1,821 participants were excluded.

Participants were also excluded if they had any pain at baseline (n = 1,342), resulting in 1,788 remaining participants. We then excluded participants that only had pain in one location at the one-year follow-up visit (n = 286). From the remaining n=1,502 participants, 115 youth had pain in at least 2 locations at the 1-year assessment. Controls were matched at a ratio of 2:1 to these new onset pain cases (n = 230). After download, it became clear that six participants (1 pain case, 5 matched controls) were missing functional images which resulted in a total of 114 children with new onset pain and 225 MCs for the resting state neural activity and functional connectivity analyses (Supplementary Fig 1).

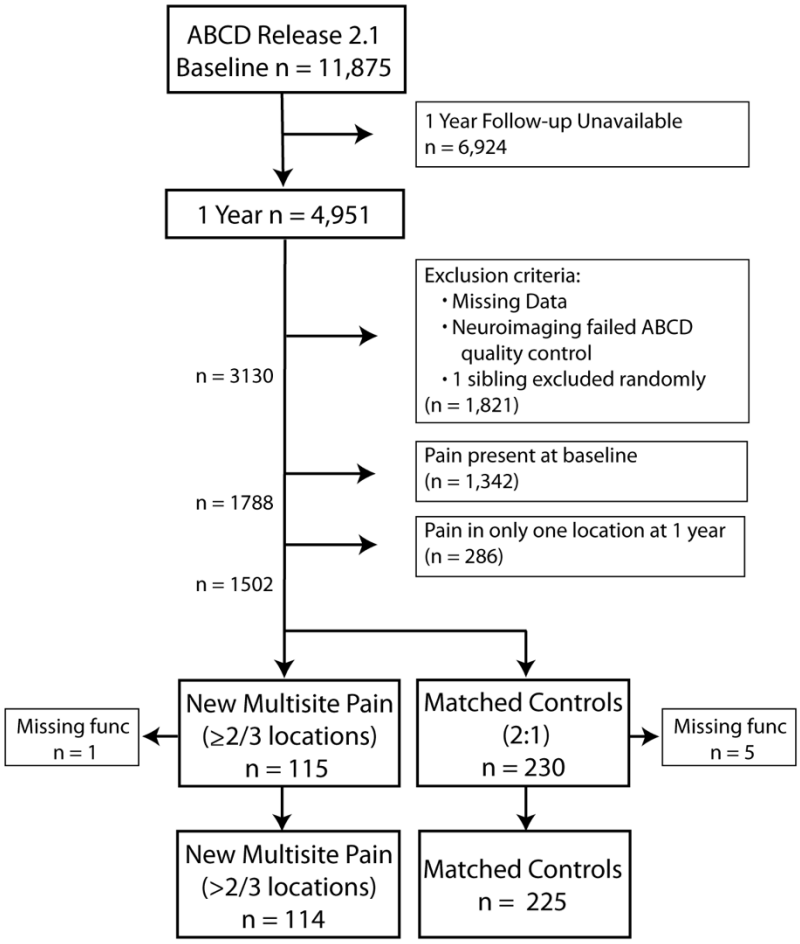

Supplementary Figure 2:
Data were checked for correlations between mean motion and functional connectivity as previously suggested (1). Before denoising, the average correlation across subjects/sessions between functional connectivity and mean motion was r = -0.08 +/- 0.06. After denoising this correlation was reduced to r = 0.01 +/- 0.06.

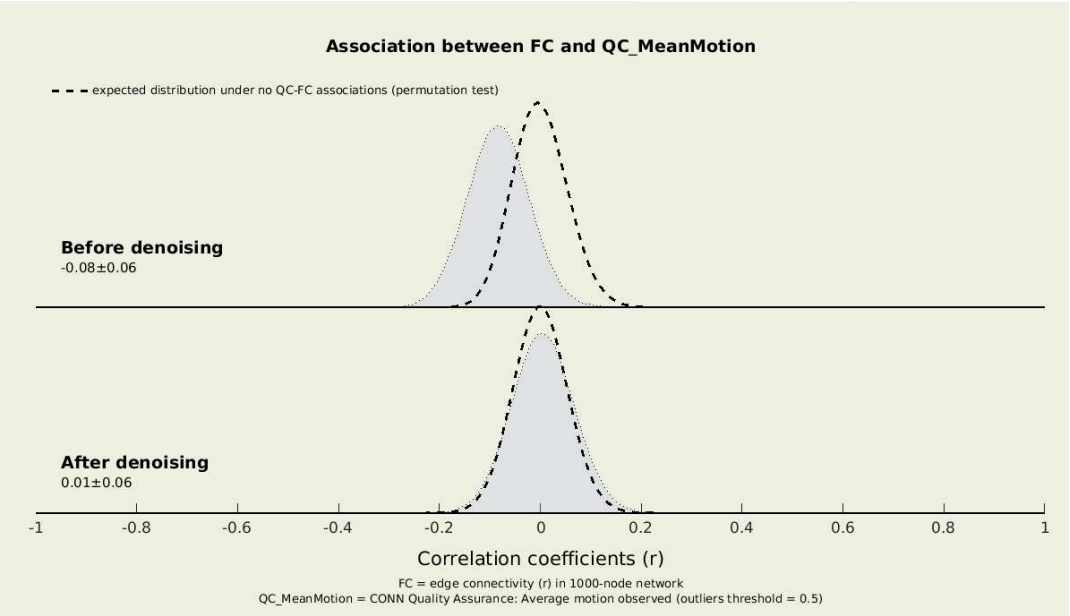

Supplementary Figure 3:
Data were checked for correlations between mean motion and functional connectivity distance dependence as previously suggested (1). Before denoising there was a strong correlation between functional connectivity and distance (r = 0.49 +/- 0.23), and after denoising this association was reduced (r = 0.01 +/- 0.19).

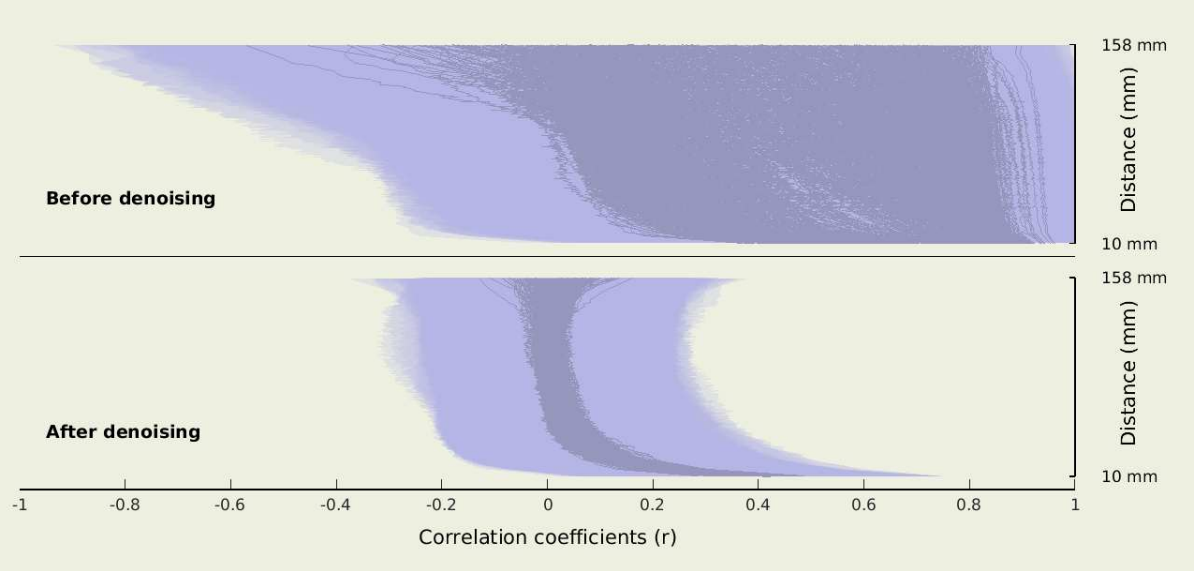

Supplementary Figure 4:
The distribution of functional connectivity values between randomly-selected brain regions before and after denoising. Before denoising, the distribution of functional connectivity values shows a pronounced positive skew and significant inter-subject variability which is indicative of physiological and motion effects. After denoising, the distribution is centered and there is reduced inter-subject variability.

Supplementary Tables

Supplementary Table 1: Baseline Demographics

	New Multisite Pain	Matched Controls	P value
sex	45.6% female	44.9% female	0.899
Pubertal status[#]	2.1 +/- .86	2.08 +/- .78	0.852
Race/ethnicity	60.5% white 10.5% black 19.3% Hispanic 0% Asian 9.6% other	61.3% white 9.3% black 19.6% Hispanic 0% Asian 9.8% other	0.989
handedness	78.9% right 5.3% left 15.8% mixed	78.2% right 5.8% left 16.0% mixed	0.979

[#] Missing data in some participants (Pain cases n = 110; Controls n = 207)

Supplementary Table 2: Coordinates for regions of interest used in functional connectivity analyses.

Region	**Coordinates**		**Ref/Source**
Anterior insula	36, 16, 2	-34, 14, 2	(6, 7)
Mid insula	38, 1, 6	-38, -1, 6	(6, 7)
Posterior insula	38, -10, 7	-38, -12, 7	(6, 7)
Thalamus	Structural ROI (bilateral)		https://www.nitrc.org/projects/wfu_pickatlas/
Amygdala	Structural ROI (bilateral)		https://www.nitrc.org/projects/wfu_pickatlas/
mPFC	2, 52, -2		(8)
Nucleus accumbens	10, 12, -8		(8)
Periaqueductal gray	1, -29, -10		(9)
dorsal ACC	-3, 32, 19		(10, 11)
Perigenual ACC	0, 40, 0		(10, 11)
Subgenual ACC	-3, 32, -8		(10, 11)

References

1. Parkes L, Fulcher B, Yucel M, Fornito A. An evaluation of the efficacy, reliability, and sensitivity of motion correction strategies for resting-state functional MRI. Neuroimage. 2018;171:415-36.
2. Avants BB, Epstein CL, Grossman M, Gee JC. Symmetric diffeomorphic image registration with cross-correlation: evaluating automated labeling of elderly and neurodegenerative brain. Med Image Anal. 2008;12(1):26-41.
3. Dale AM, Fischl B, Sereno MI. Cortical surface-based analysis. I. Segmentation and surface reconstruction. Neuroimage. 1999;9(2):179-94.
4. Zhang Y, Brady M, Smith S. Segmentation of brain MR images through a hidden Markov random field model and the expectation-maximization algorithm. IEEE Trans Med Imaging. 2001;20(1):45-57.
5. Ashburner J, Friston KJ. Voxel-based morphometry--the methods. Neuroimage. 2000;11(6 Pt 1):805-21.
6. Taylor KS, Seminowicz DA, Davis KD. Two systems of resting state connectivity between the insula and cingulate cortex. Hum Brain Mapp. 2009;30(9):2731-45.
7. Ichesco E, Schmidt-Wilcke T, Bhavsar R, Clauw DJ, Peltier SJ, Kim J, et al. Altered resting state connectivity of the insular cortex in individuals with fibromyalgia. J Pain. 2014;15(8):815-26 e1.
8. Baliki MN, Petre B, Torbey S, Herrmann KM, Huang L, Schnitzer TJ, et al. Corticostriatal functional connectivity predicts transition to chronic back pain. Nat Neurosci. 2012;15(8):1117-9.
9. Linnman C, Moulton EA, Barmettler G, Becerra L, Borsook D. Neuroimaging of the periaqueductal gray: state of the field. Neuroimage. 2012;60(1):505-22.
10. Schmidt-Wilcke T, Ichesco E, Hampson JP, Kairys A, Peltier S, Harte S, et al. Resting state connectivity correlates with drug and placebo response in fibromyalgia patients. Neuroimage Clin. 2014;6:252-61.
11. Bingel U. [Mechanisms of endogenous pain modulation illustrated by placebo analgesia : functional imaging findings]. Schmerz. 2010;24(2):122-9.